How to cite: *Angew. Chem. Int. Ed.* **2020**, *59*, 12048–12054
International Edition: doi.org/10.1002/anie.202002951
German Edition: doi.org/10.1002/ange.202002951

Aerogels

Tailoring the Morphology and Fractal Dimension of 2D Mesh-like Gold Gels

*Karl Hiekel, Swetlana Jungblut, Maximilian Georgi, and Alexander Eychmüller**

Abstract: *As there is a great demand of 2D metal networks, especially out of gold for a plethora of applications we show a universal synthetic method via phase boundary gelation which allows the fabrication of networks displaying areas of up to 2 cm^2. They are transferred to many different substrates: glass, glassy carbon, silicon, or polymers such as PDMS. In addition to the standardly used web thickness, the networks are parametrized by their fractal dimension. By variation of experimental conditions, we produced web thicknesses between 4.1 nm and 14.7 nm and fractal dimensions in the span of 1.56 to 1.76 which allows to tailor the structures to fit for various applications. Furthermore, the morphology can be tailored by stacking sheets of the networks. For each different metal network, we determined its optical transmission and sheet resistance. The obtained values of up to 97 % transparency and sheet resistances as low as 55.9 Ω/sq highlight the great potential of the obtained materials.*

Introduction

2D gold structures, such as meshes and networks, are used in a multiplicity of applications, namely flexible electrodes for biomedical applications like neural implants or in real-time monitoring of cells or blood vessels,[1–3] micro- and nano-electromechanical systems (NEMS/MEMS) to detect or respond to the presence of chemical vapors or gases,[4,5] electronic skins[5,6] and many more.[7–10] Hence, there is a great interest and demand to have an easy synthesis approach and possibilities to tailor the 2D gold structures according to their intended applications. The terminology used to refer to these 2D structures is not uniform since it is usually related to the respective synthesis route used to fabricate them. The established synthesis routes include Langmuir–Blodgett-type methods,[11] UV irradiation,[12] nanoimprinting,[13] dealloying,[14] and phase boundary gelation[15–18] with more of them were presented in the literature the last years.[9] The structures formed are named cluster aggregates,[11] nanoframeworks,[18] or nanowires[7,15] to mention some and often the 2D character of these structures is stressed as the lateral dimensions are by far larger than the thicknesses. Herein, we use a phase boundary gelation method to synthesize a gold network structure (also called 2D mesh-like gold (aero)gel)) out of Au nanoparticles (NPs). Noble metal aerogels were developed in 2009 by our group.[19] In the here presented phase boundary gelation method, a solution with electrostatically stabilized nanoparticles is brought in contact with another solution, which destabilizes the particles such that they can approach each other and stick together irreversibly, that is, gelate on the timescale of an experiment (within seconds). Hence, the particles diffusing through the phase boundary into the second solution self-assemble into a disordered structure similar to those obtained via reaction-limited cluster aggregation (RLCA) and diffusion-limited cluster aggregation (DLCA).[20–22] A direct comparison with the models, which predict the formation of network structures with fractal dimensions between 1.45 (DLCA) and 1.53 (RLCA), is, however, unreasonable due to the fact that their basic assumption of the rigid inter-particle bonds forming irreversibly is not supported in our case of rather flexible networks. In the same time, the observed similarity of the structures indicates that the key parameters that control the structure formation have to be related to the factors that regulate the sticking probability between the diffusing particles as well as the stiffness of the chains in the forming structure. The identification of all these parameters is rather difficult. Nevertheless, self-assembly of particles is a fascinating process[23] which is often employed in the synthesis of (metal) aerogels.[24,25] A number of recent studies on 3D metal aerogels explored routes for the direct morphology control.[26,27] Herein, we further investigate synthetic options to tailor the morphology of metal networks in 2D and fine-tune them for specific applications.

In addition, we pay particular attention to the fractal dimension of the obtained gels. On the length scale set by the web thickness, the fractal dimension provides a measure for the similarity of the networks. Furthermore, a decrease of the fractal dimension is associated with the decrease of the gel density and hence the appearance of larger holes in the gel structure. The main specifications commonly used to characterize aerogels, which are their web thicknesses (also sometimes named and identical with wire diameters or ligament sizes) and (specific) surface area, do not give any direct information about how effectively a structure fills the space, which is provided by the fractal dimension. We apply the box-counting algorithm to determine the fractal dimension of the formed gels.[28] Our 2D structures can easily be analyzed using

[*] K. Hiekel, Dr. S. Jungblut, M. Georgi, Prof. Dr. A. Eychmüller
Physical Chemistry
Technische Universität Dresden
Bergstrasse 66b, 01062 Dresden (Germany)
E-mail: alexander.eychmueller@chemie.tu-dresden.de
Supporting information and the ORCID identification number(s) for the author(s) of this article can be found under: https://doi.org/10.1002/anie.202002951.

electron microscopy like SEM or TEM, which allows a comparison between the morphologies of different structures. The standard analysis of metal aerogel morphologies usually neglects the value of fractal dimension partially because its determination in 3D is rather complex. In this contribution, we demonstrate the suitability and potential of the concept of fractal dimension to characterize 2D mesh-like gels. In addition, the synthesis route is quite fast as it is finished within minutes and the obtained 2D gels can easily be transferred to many kinds of substrates such as glass, silica, glassy carbon, or polymers, such as PDMS. Through variation of experimental conditions, we explore the possibilities how to tailor the morphology of metal aerogels and use fractal dimension as an additional parameter to characterize their structures.

Results and Discussion

The route we followed to prepare 2D mesh-like gold gels on a substrate of choice is sketched in Figure 1 a. First, a drop of freshly prepared aqueous Au NP solution is placed onto a glass substrate (step I; Figure 1 a). Then, it is overlaid with an organic solvent mixture (step II; Figure 1 a). To maintain the phase boundary, the mixture consisted of EtOH and toluene as EtOH is soluble in both media, namely toluene and way better in water. Bringing the organic and aqueous solutions in contact causes their mixing in which EtOH functions as a mediation solvent that transports the charge stabilized Au NPs[29] into the organic phase. Observations showed that passing the phase boundary to EtOH is easily possible for Au NPs. During the mixing process, Au NPs diffuse into the EtOH-rich regions of the organic phase while the amount of EtOH in the organic phase depletes as it diffuses into the aqueous phase leaving the Au NPs in the organic one. This leads to the gelation of the Au NPs into a network structure at the phase boundary as here the dielectric constant changes abruptly from 80.35 in the aqueous phase to 2.4 in the toluene phase (step III; Figure 1 a). The particles cannot diffuse deeper into that phase and have only two directions of aggregation left forming 2D islands of gold network structures. The formation mechanism of larger network structures is analogous to the mechanism shown by Chauvin et al.[14] The islands of the network structures in the organic compound diffuse around. By contact, they fuse together into larger ones until a single 2D gel with a size up to 2 cm^2 (see also image Figure 1 b) is reached, eventually. The process can be observed visually. However, it proceeds too fast to be quantitatively analyzed by simple means. Hence, for a deeper insight a separate investigation would be needed. The SEM image in Figure 1 c reveals that flawless areas with nearly no visible surface defects are formed. However, this was not always the case as small cracks as also described by Chauvin and co-workers[14] could sporadically also be found (see Supporting Information Figure S1 and S2). The diffusion of the islands on top of the water phase stops after the evaporation of the organic layer. As a result of the hydrophobic character of the gold structure (as is claimed in the literature for similar experiments[14,15]) and/or the surface tension of water, the network structure does not sink in but stays clearly visible on the surface of the drop after the organic phase has evaporated. It then can easily be transferred if a substrate is stamped onto the Au network structure (step IV of Figure 1 a). As stamps several materials can be used like glass, glassy carbon, PDMS, Si-wafer or others depending on the desired application. SEM and TEM images of the obtained network structures (Figure 1 d, e) reveal that a flat network structure is achieved regardless to which substrate the network structure was transferred. Additionally, AFM measurements on a silica wafer as substrate

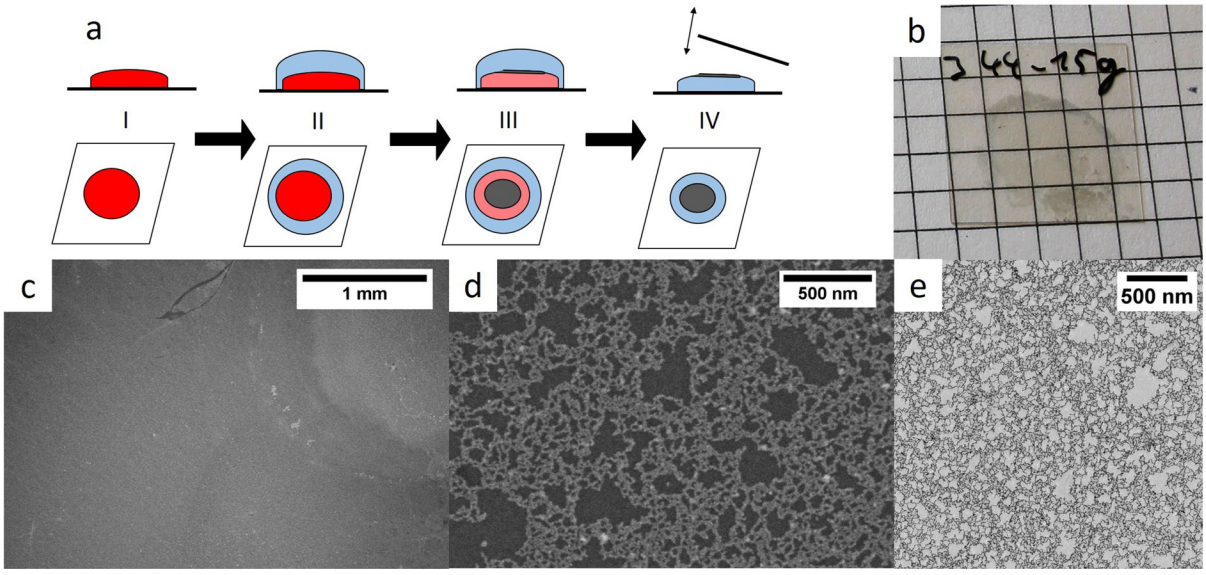

Figure 1. a) Schematic overview of 2D gold network structure synthesis and its transfer, top row: side view, bottom row: top view; red initial aqueous Au NP solution, light blue organic/aqueous solvent containing no Au NPs, light red aqueous phase containing lesser Au NPs, gray 2D gold network structure; b) a 2D gold network structure on a glass slide (1 square equals 0.25 cm^2); c),d) SEM images of 2D gold network structure on glassy carbon substrate; e) TEM image of 2D gold network structure.

(can be found in SI 3) showed that the height and the width of the wires were similar which indicates a cylindrical shape of the wires. A transfer of the network structure to a substrate prevents its contamination. Waiting till both the organic and the aqueous solutions evaporate infers the formation of byproducts like salt crystals that distort the structure of the gel. In principle, those can be removed by washing, however, inhomogeneities will remain in the 2D gel structure. For more details see SI 4 where a 2D gel structure damaged due to the presence of a salt crystal is shown. In addition, we also show an image in which agglomerates of non gelated Au NPs accumulated within the gel structure. It was not possible to remove them afterwards.

To produce 2D gold gels, we used a 1:1 mixture of EtOH and toluene. We note in passing that an earlier work on the self-assembly of gold NPs into networks it was stated that toluene is crucial for the synthesis as it passivates the gold surfaces to form smooth wires.[15] However, we found that the synthesis also works well with pure EtOH. In this case, the amount of EtOH has to be quite large as it is easily miscible with water. A detailed description of the process, more characteristics and other side experiments related to this can be found in Figure S5 and S6.

Interestingly, these syntheses strategies can in principle also be used for other elements such as Ag, Pd, and Pt, showing the versatility of these methods. Whereby the Ag gel is synthesized by overlaying the NP solution with EtOH and gently shaking it and the Pd and Pt gels are gained by overlaying their NP solutions with the toluene/EtOH mixture (more details are given in the experimental section in the Supporting Information). TEM images of those 2D gel structures are displayed in Figure S7.

In the following, we examine the details of the morphology of the mesh-like gel structures (gelated using the toluene/EOH mixture) which we influenced and tailored by the variation of the ratio of reducing agent to metal precursor (for details see experimental section in the Supporting Information). Table 1 presents a summary of the results in terms of quantities and physical properties. Already a visual inspection of the TEM images in Figure 2a–d reveals that four different kinds of structures were achieved with four different ratios of reducing agent to metal precursor. The web thickness is largest at very low and very high ratios and tends to be on a minimum plateau in between. Explaining these trends is rather difficult. The size difference of the Au NPs is probably not the key factor as a visual analysis of the respective TEM images reveals that the Au NP size differences are quite small. The initial size of the Au NPs does not depend on the ratio of reducing agent to metal precursor but on the amount of additionally added supplementary ions (which were not added in our synthesis procedure).[29] Nevertheless, if a higher ratio of reducing agent to metal precursor is used, metal NPs are longer stabilized and more negatively charged at the surface and the reducing agent $NaBH_4$ increases the pH value.[29,30] A change of the electrostatic forces of the NPs is necessary to influence the self-assembly.[31] Several studies describe factors which influence the electrostatic forces and therefore the self-assembly like pH value, surface charge, or solvent but a generalizing theory for precisely controlling self-assembly and gelation is still missing.[32–35] Also, the pH value and the charge of the NPs influence the attachment at the phase boundary between the liquids which should also influence the gelation.[36,37] The change of the $NaBH_4$ concentration affects many of these described factors. Whether it is a combination of those factors and which of those are the main contributors is not yet fully clear, so that a deeper investigation is needed. Only in recent times first detailed attempts were made to control the web thickness of noble metal aerogels in a broad range.[26,27] Changing the ratio of reducing agent to precursor to even lower or higher values as shown in our experiments is unrewarding as the percolation of the overall structure will be incomplete. For more information see also Figure S8.

For further usage, it is desirable to have large continuous network structures. Therefore, the average size of the network structures obtained was also analyzed photographically. Initially, the upper limit is approximately 1 cm^2 and follows an inverse trend compared to the web thickness. The most obvious method to increase the network structure size is to use larger volumes of Au NP solution for the phase boundary gelation. The parameters of the network structures obtained with the initial amount of the Au NP solution doubled are

Table 1: Overview of results for different samples showing average web thickness, fractal dimension, surface coverage within a network, transmission values at 550 nm for one to three monolayers (ML), sheet resistance values for one to three monolayers, ratio of network size to drop size, average area of the network, for samples produced using respective amounts of $NaBH_4$: **2** (2 mL), **3** (3 mL), **4** (4 mL), **5** (5 mL). The difference between samples **a** and **b** is the amount of Au NP solution used for gelation, which was 200 μL and 400 μL, respectively.

Property	Unit	Sample							
		2a	**2b**	**3a**	**3b**	**4a**	**4b**	**5a**	**5b**
Web thickness	nm	9.0	14.7	4.3	5.1	4.3	4.8	5.6	4.1
Fractal dimension		1.762	1.656	1.580	1.641	1.674	1.705	1.712	1.559
Coverage on nanoscale		0.494	0.31	0.252	0.333	0.402	0.449	0.364	0.231
Transmission 1 ML	%	88.91	90.86	96.15	94.39	94.54	95.98	92.8	96.66
Transmission 2 ML	%	79.88	82.33	90.17	89.69	88.38	91.74	86.82	92.54
Transmission 3 ML	%	69.73	77.87	85.67	79.4	80.57	86.65	79.34	88.07
Resistance 1 ML	Ω/sq	–	–	359	65.96	366	548.22	197.33	269.85
Resistance 2 ML	Ω/sq	165.66	–	156	236.96	165.93	98.53	97.71	72.03
Resistance 3 ML	Ω/sq	148.09	–	94.68	55.9	55.36	125.53	81.45	73.97
Coverage compared to drop size		0.213	0.206	0.481	0.472	0.488	0.629	0.360	0.589
Average size of network structure	mm^2	46.1	64.2	104.1	147.1	105.6	196.1	77.9	183.5

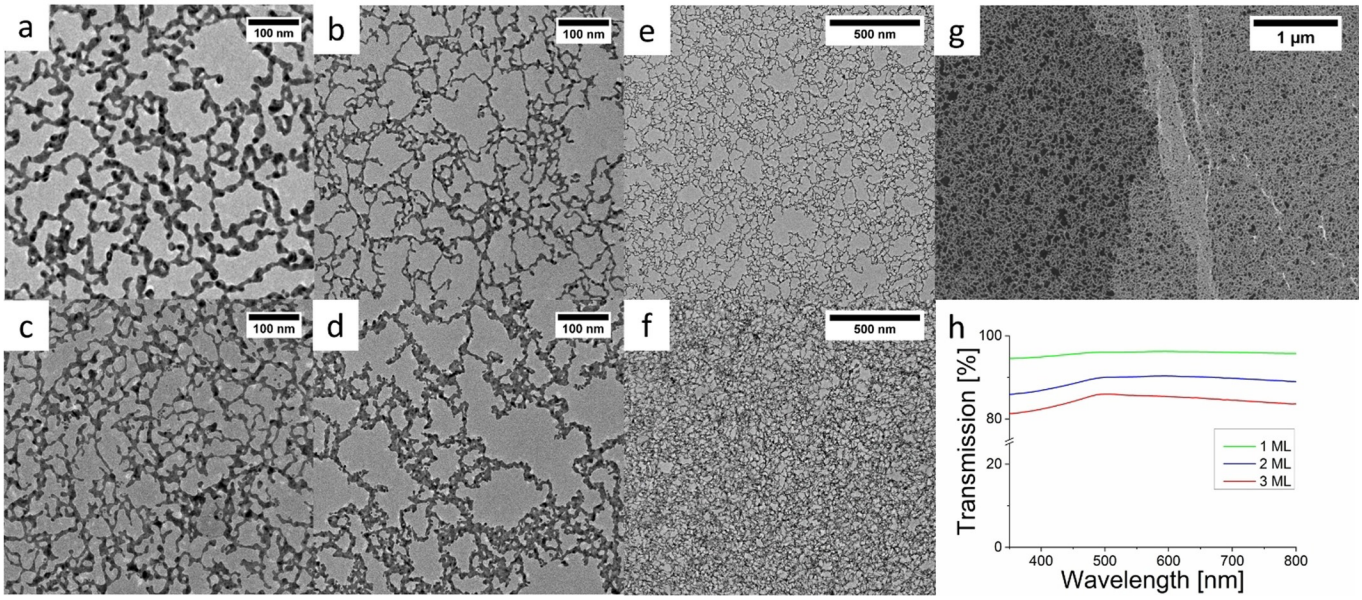

Figure 2. TEM images of 2D gold network structures produced using 200 µL of Au NP solution synthesized with 2 mL (a), 3 mL (b), 4 mL (c), and 5 mL (d) of $NaBH_4$ solution; TEM images of non-stacked (e) and stacked (f) 2D gold network structures of sample **3a**; g) SEM image of the boundary between non-stacked and stacked 2D gold network structures using sample **3a**; h) transmission spectra of sample **3a** with one to three monolayers (ML).

summarized in Table 1 and labeled with **b** (samples with the starting parameters are labeled with **a**), while TEM images of these samples are located in Figure S9. Interestingly, not only the network structure size increased to nearly 2 cm^2 (for samples using higher ratios of reducing agent to metal precursors (i.e. samples **4b** and **5b**) the values on average are smaller) but also the web thickness and fractal dimension changed. This observation leads to the conclusion that the amount of material used is one of the parameters to influence the morphology.

As mentioned above, the fractal dimension gives insight about the effectiveness, with which a structure fills the space. Hence, the lower that value gets the less dense the network structures become. Considering that the web thickness only sets the scale of a fractal structure, the change of the fractal dimension is associated with an increase of the "hole sizes' of the mesh-like gels. Gels **3a**, **4a**, **4b** (Table 1) have the same web thickness but different fractal dimensions. This means that the density of the gel structures, and, hence the size of the holes in the networks are different. Gels **2b** and **3b** display nearly the same fractal dimension which means that their network structure is quite similar. Their web thickness, however, is significantly different indicating that the gels are self-similar to each other with just a different scaling factor. These examples impressively show the possibility to tailor such network structures. In this order of magnitude, it is a novelty and contributes to a better understanding how to experimentally influence the gelation process and how to precisely describe gel networks. By variation of the reducing agent to metal precursor ratio, we were able to change the web thickness between 4.1 nm and 14.7 nm and the fractal dimension between 1.559 and 1.762. The theory of diffusion-limited cluster aggregation predicts that the fractal dimension of 2D structures can be as low as 1.45.[21,38] Indeed, we found this value for some of the Au gels presented here (see Figure S10). The fractal dimension of the majority of the structures lies, however, above this value and also above the value of 1.53 predicted for RLCA.[22] We attribute the differences mainly to the flexibility of the obtained structures but cannot rule out the influence of other factors like the restructuration of the NPs or their networks. Nevertheless, the similarity of the structures suggests that the analytical conclusions might qualitatively apply in our case. For instance, we can verify the fact that the morphology of our networks is largely independent on the NP concentration, as suggested by DLCA and RLCA.[21,39] On the one hand, diluting the NP solution of sample 3a by 20%, which is the lowest concentration above which we still could find interconnected networks, had a relatively small impact on the network structure with a web thickness of 3.8 nm (compared to 4.3 nm) and fractal dimension of 1.533 (compared to 1.580). Increasing the NP concentration, on the other hand, caused their fast agglomeration into larger NPs as no stabilizers were present. Furthermore, if the particle size became too large, the phase boundary gelation did not take place. Hence, at the very low particle concentrations considered here it is highly probable that the particle density is one of the less important factors affecting the structure. For this reason, we conclude that altering the ratio of reducing agent to metal precursor had the largest impact on the synthesized structures.

Not only the nanoscopic properties but also the macroscopic ones like the network structure size are of interest. The network structure formation works best with using a relatively high volume of the Au NP solution and high ratios of reducing agent to metal precursor (i.e. samples **4b** and **5b**) where the obtained network structures cover the largest area of nearly

2 cm^2 on average and show a minimum amount of defects. In contrast, the synthesis routes using the lowest ratio of reducing agent to metal precursor (i.e. samples **2a** and **2b**) result only in the formation of network structures that are highly crumpled, which hampers their further use. In principle, it is possible to estimate the size of a fractal structure from its fractal dimension and the amount of material used to produce it. In Supporting Information Section 11, we sketch the respective derivation, where the mass of a fractal aggregate is linked with the fractal dimension and mass and size of a single NP.[40] This approach overestimates the size of ideal network structures in comparison to reality. One of the main reasons for this discrepancy is the imperfection of the macroscopic network structure, namely the occurrence of multilayers and the fact that usually a small fraction of Au NPs is not incorporated into the network. Sometimes, small cracks within the network structure can be found (see also Figure S1) for which at least three reasons might be considered. First, in the course of the diffusion and fusion of the mesh-like islands not all parts interconnect well which leaves partial small spaces open. Second, the mesh transfer causes stress to the structure which might favor crack formation. Third, the drying process on air is generally harmful for gel structures as the pores collapse. Certainly, further developments will lead to network structure formation and network structure transfer methods with less defects and larger uniform mesh-like gels.

To overcome the deficiencies already today we stacked several layers of network structures on top of each other. Statistically, it is very unlikely that two cracks completely overlap and hence the defects appearing in one of the mesh-like gels will be compensated by the structure of the others. Herein, we examine stacks of up to three layers of Au mesh-like gels with all of the investigated network topologies. Details of their preparation and the stacking procedure are presented in the experimental section of the Supporting Information. In principle, there is no limitation for the number of stacked layers although the 2D character of the material will eventually be lost. Figure 2 shows TEM photographs of the non-stacked (Figure 2e) and stacked (Figure 2f) network structures together with an SEM image (Figure 2g) of a network structure and its overlap with a second network structure. In the samples shown in Figure 2e, f, the fractal dimensions as well as the covered areas of the newly formed network increase from 1.53 to 1.73 and from 34% to 50%, respectively with an additional layer. As expected, there is no change in web thickness. Figure 2g demonstrates that the edges of the structure tend to wrinkle up as it is no surprise that the edges can easily loose the contact to the substrate. With a functionalization of the substrate surface these phenomena should be prevented. The stacking method is an additional possibility to tailor the network structures as it modifies the network structure hole sizes and bridges cracks in the overall structure keeping the web thickness constant. With the options to change the morphology and stack multiple layers, network structures can be synthesized and fine-tuned to fulfill the particular requirements for different devices.

The value of sheet resistance is important to evaluate the effectiveness of a material for further applications, for instance as electrodes or sensors. These results for all samples are presented in Table 1. The expectation that the sheet resistance will decrease with each additional stack because cracks and irregularities will be overbridged is met by the samples in which the smaller volume of Au NP solution was used (i.e. samples **2a**, **3a**, **4a**, **5a**). For those, the sheet resistances drop with each successive layer. For the other samples where a larger volume of Au NP solution was used the macroscopic network structure integrity is more intact meaning that less defects appear within the layers. Especially, a relatively low value of the sheet resistance of the one monolayer of sample **3b** indicates a mesh-like gel nearly without damages or irregularities. The same applies for two monolayers of sample **5b**, where an additional layer causes even an increase in sheet resistance which indicates a layered structure with more defects than in a single monolayer. The tendency to form cracks seems to be lower for the larger sized mesh-like gels. The reason why this behavior is different compared to the samples using the smaller volumes of Au NP solution still has to be unraveled.

Gold nanostructures show plasmonic features and can therefore interact with light. As an example, transmission spectra of sample **3a**, which showed the highest transparency of all samples, are presented in Figure 2c. The spectra measured for the other samples can be found in Figure S12. An overview of all the values is displayed in Table 1. In one layer of network structure, the values reach from 89.0% to 96.7% transmission. As mentioned above, the stacking of mesh-like gels bridges possible cracks which increases the integrity of the network structure and, therefore, boosts its conductivity in most cases. Of course, the transmission decreases with each additional layer. In fact, the transmission drops between around 4 percentage points and 10 percentage points per additional layer and follows a nearly linear trend for each set of synthesis parameters. In general, transmission values are linked to the coverage and therefore to the fractal dimension as those values are also linked (see Figure S13). The majority of the results indicates that, as expected, the transmission increases with the decrease of the coverage. However, there remain two outliers even after repeated experiments, which do not follow this trend, namely samples **2b** and **4b**. As described earlier, in sample **2b**, the single layers of networks tend to wrinkle up and lower the transmission since these wrinkles show a larger absorption. However, it was possible to find flat areas on the TEM images, which allowed to determine the fractal dimension of those structures. In contrast, the blank areas within the networks of sample **4b** originating from a large number of cracks resulting in a higher transmission in this case. The explanation of plasmonic features for non-ordered structures is still a great challenge. Further investigations are under way to provide an interpretation of these phenomena.

The samples presented here display a large range of transparencies and sheet resistances which are comparable and, in some cases, excel the performance of 2D gold structures synthesized earlier. In a previous study, ordered network structures of gold nanowires were printed on glass

and show a transmission of 92% (at 500 nm) with a sheet resistance of 227 Ω/sq (15 nm web thickness) or 68% transmission (at 500 nm) with 29 Ω/sq (45 nm web thickness).[13] With a transmission of 94% and sheet resistance of 66 Ω/sq we were able to improve the transparency but could not reach the same sheet resistance. The best figure of merit (Haacke) was achieved for sample **3b**/1 ML with 0.0085 Ω^{-1} (other data are presented in Figure S14).[41] To our knowledge, only one study considered 2D fractal gold networks.[18] They show wires with a web thickness of 20 nm diameter and transmission and sheet resistance of 70% (550 nm) and 100 Ω/sq, respectively. The fractal dimension was 1.9 which is quite high and indicates rather dense structures. Additional results for comparison of sheet resistance and transmission can be found in the literature.[5] To estimate whether the here synthesized network structures can be an alternative to the commonly used indium tin oxide (ITO) its values have to be met. ITO shows transparencies of 80% till 95% and sheet resistances up to as low as 5 Ω/sq.[42] Compared, the gold network structures still lack behind the sheet resistance values despite they both are in the same region for transparency. Nevertheless, gold structures show a much better flexibility than ITO and have therefore a different and broader scope of application. In addition, the proposed synthesis route and transfer of the mesh-like gels provide an easy and fast approach with plenty of options to tailor the networks for further use.

Conclusion

We showed a new synthesis method to easily fabricate and tailor 2D Au gel structures with areas of up to 2 cm^2. The variation of experimental parameters allowed us to synthesize a multiplicity of different network structures with fractal dimensions in the range of 1.559 to 1.762 and web thicknesses between 4.1 nm and 14.7 nm. Furthermore, we have shown that stacking them is a feasible tool to tailor the morphology of the structure. Additionally, we measured the transmission and the sheet resistance demonstrating that the mesh-like gels with 97% transmission and 55.9 Ω/sq sheet resistance are comparable to the state-of-the-art analogues described in the literature but prepared in an easier and faster way. Further investigations will focus on the mechanical stability and flexibility of these network structures. As also shown, the use of other metals, such as Ag, Pd, and, Pt (and their alloys), for this kind of phase boundary gelation is straightforward facilitating their tailoring and fine-tuning for further applications.

Acknowledgements

We acknowledge the help of Bendix Ketelsen by performing the AFM measurements and Christoph Bauer with additional support for SEM measurements. We acknowledge the financial support from the European Research Council (ERC AdG AEROCAT no. 340419), the Swiss National Science Foundation and the German Research Foundation (DFG EY 16/18-2).

Conflict of interest

The authors declare no conflict of interest.

Keywords: 2D structures · aerogels · fractal structures · gold

[1] I. R. Minev, P. Musienko, A. Hirsch, Q. Barraud, N. Wenger, E. M. Moraud, J. Gandar, M. Capogrosso, T. Milekovic, L. Asboth, et al., *Science* **2015**, *347*, 159 – 163.
[2] Y. Liu, M. Pharr, G. A. Salvatore, *ACS Nano* **2017**, *11*, 9614 – 9635.
[3] Y.-L. Liu, Z.-H. Jin, Y.-H. Liu, X.-B. Hu, Y. Qin, J.-Q. Xu, C.-F. Fan, W.-H. Huang, *Angew. Chem. Int. Ed.* **2016**, *55*, 4537 – 4541; *Angew. Chem.* **2016**, *128*, 4613 – 4617.
[4] H. Schlicke, M. Behrens, C. J. Schröter, G. T. Dahl, H. Hartmann, T. Vossmeyer, *ACS Sens.* **2017**, *2*, 540 – 546.
[5] S. Huang, Y. Liu, C. F. Guo, Z. Ren, *Adv. Electron. Mater.* **2017**, *3*, 1600534.
[6] Y. Wang, S. Gong, S. J. Wang, X. Yang, Y. Ling, L. W. Yap, D. Dong, G. P. Simon, W. Cheng, *ACS Nano* **2018**, *12*, 9742 – 9749.
[7] K. Kim, Y. Park, B. G. Hyun, M. Choi, J. Park, *Adv. Mater.* **2019**, *31*, 1804690.
[8] R. Dong, T. Zhang, X. Feng, *Chem. Rev.* **2018**, *118*, 6189 – 6235.
[9] B. Zhu, S. Gong, W. Cheng, *Chem. Soc. Rev.* **2019**, *48*, 1668 – 1711.
[10] J. Lv, K. Hou, D. Ding, D. Wang, B. Han, X. Gao, M. Zhao, L. Shi, J. Guo, Y. Zheng, et al., *Angew. Chem. Int. Ed.* **2017**, *56*, 5055 – 5060; *Angew. Chem.* **2017**, *129*, 5137 – 5142.
[11] T. Reuter, O. Vidoni, V. Torma, G. Schmid, L. Nan, M. Gleiche, L. Chi, H. Fuchs, *Nano Lett.* **2002**, *2*, 709 – 711.
[12] W. Tong, S. Yang, B. Ding, *Colloids Surf. A* **2009**, *340*, 131 – 134.
[13] J. H. M. Maurer, L. González-García, B. Reiser, I. Kanelidis, T. Kraus, *Nano Lett.* **2016**, *16*, 2921 – 2925.
[14] A. Chauvin, W. Txia Cha Heu, J. Buh, P.-Y. Tessier, A.-A. El Mel, *npj Flexible Electron.* **2019**, 3.
[15] G. Ramanath, J. D'Arcy-Gall, T. Maddanimath, A. V. Ellis, P. G. Ganesan, R. Goswami, A. Kumar, K. Vijayamohanan, *Langmuir* **2004**, *20*, 5583 – 5587.
[16] S. Gao, H. Zhang, X. Liu, X. Wang, L. Ge, *J. Colloid Interface Sci.* **2006**, *293*, 409 – 413.
[17] S. C. Yang, X. W. Wan, Y. T. Ji, L. Q. Wang, X. P. Song, B. J. Ding, Z. M. Yang, *CrystEngComm* **2010**, *12*, 3291 – 3295.
[18] M. D. Ho, Y. Liu, D. Dong, Y. Zhao, W. Cheng, *Nano Lett.* **2018**, *18*, 3593 – 3599.
[19] N. C. Bigall, A. K. Herrmann, M. Vogel, M. Rose, P. Simon, W. Carrillo-Cabrera, D. Dorfs, S. Kaskel, N. Gaponik, A. Eychmüller, *Angew. Chem. Int. Ed.* **2009**, *48*, 9731 – 9734; *Angew. Chem.* **2009**, *121*, 9911 – 9915.
[20] M. Kolb, R. Botet, R. Jullien, *Phys. Rev. Lett.* **1983**, *51*, 1123 – 1126.
[21] P. Meakin, *Phys. Rev. Lett.* **1983**, *51*, 1119 – 1122.
[22] R. Jullien, M. Kolb, *J. Phys. A* **1984**, *17*, https://doi.org/10.1088/0305-4470/17/12/003.
[23] G. M. Whitesides, *Science* **2002**, *295*, 2418 – 2421.
[24] B. Cai, V. Sayevich, N. Gaponik, A. Eychmüller, *Adv. Mater.* **2018**, *30*, 1707518.
[25] F. Rechberger, M. Niederberger, *Nanoscale Horiz.* **2017**, *2*, 6 – 30.
[26] M. Georgi, B. Klemmed, A. Benad, A. Eychmüller, *Mater. Chem. Front.* **2019**, *3*, 1586 – 1592.

[27] R. Du, Y. Hu, R. Hübner, J.-O. Joswig, X. Fan, K. Schneider, A. Eychmüller, *Sci. Adv.* **2019**, *5*, eaaw4590.
[28] S. R. Forrest, T. A. Witten, *J. Phys. A* **1979**, *12*, L109 – L117.
[29] M. Wuithschick, S. Witte, F. Kettemann, K. Rademann, J. Polte, *Phys. Chem. Chem. Phys.* **2015**, *17*, 19895 – 19900.
[30] D. L. Van Hyning, C. F. Zukoski, *Langmuir* **1998**, *14*, 7034 – 7046.
[31] Y. Min, M. Akbulut, K. Kristiansen, Y. Golan, J. Israelachvili, *Nat. Mater.* **2008**, *7*, 527 – 538.
[32] Z. Zhang, Y. Wu, *Langmuir* **2010**, *26*, 9214 – 9223.
[33] S. Lin, M. Li, E. Dujardin, C. Girard, S. Mann, *Adv. Mater.* **2005**, *17*, 2553 – 2559.
[34] H. Zhang, K. H. Fung, J. Hartmann, C. T. Chan, D. Wang, *J. Phys. Chem. C* **2008**, *112*, 16830 – 16839.
[35] R. Du, J. Wang, Y. Wang, R. Hübner, X. Fan, I. Senkovska, Y. Hu, S. Kaskel, A. Eychmüller, *Nat. Commun.* **2020**, *11*, 1590.
[36] F. Reincke, S. G. Hickey, W. K. Kegel, D. Vanmaekelbergh, *Angew. Chem. Int. Ed.* **2004**, *43*, 458 – 462; *Angew. Chem.* **2004**, *116*, 464 – 468.
[37] F. Reincke, W. K. Kegel, H. Zhang, M. Nolte, D. Wang, D. Vanmaekelbergh, H. Möhwald, *Phys. Chem. Chem. Phys.* **2006**, *8*, 3828 – 3835.
[38] P. Meakin, Z. R. Wasserman, *Phys. Lett. A* **1984**, *103*, 337 – 341.
[39] S. Jungblut, J.-O. Joswig, A. Eychmüller, *Phys. Chem. Chem. Phys.* **2019**, *21*, 5723 – 5729.
[40] P. Meakin, *Fractals, Scaling and Growth Far from Equilibrium*, Cambridge University Press, Cambridge, **1997**.
[41] G. Haacke, *J. Appl. Phys.* **1976**, *47*, 4086 – 4089.
[42] D. H. Wang, A. K. K. Kyaw, V. Gupta, G. C. Bazan, A. J. Heeger, *Adv. Energy Mater.* **2013**, *3*, 1161 – 1165.

Manuscript received: February 26, 2020
Accepted manuscript online: April 21, 2020
Version of record online: May 18, 2020

